Point Contact Andreev Reflection Studies on Superconductors

Preetha Saha

A dissertation submitted for the partial fulfilment of BS-MS dual degree in Science

Indian Institute of Science Education and Research Mohali

April, 2015

Certificate of Examination

This is to certify that the dissertation titled **Point Contact Andreev Reflection Studies on Superconductors** submitted by **Ms. Preetha Saha** (Reg. No. MS10024) for the partial fulfilment of BS-MS dual degree programme of the Institute, has been examined by the thesis committee duly appointed by the Institute. The committee finds the work done by the candidate satisfactory and recommends that the report be accepted.

Dr. Sanjeev Kumar Dr. Yogesh Singh Dr. Goutam Sheet

(Supervisor)

Dated: April 22, 2015

Declaration

The work presented in this dissertation has been carried out by me under the guidance of Dr. Goutam Sheet are involved, every effort is made to indicate this clearly, with due acknowledgement of collaborative research and discussions. This thesis is a bonafide record of original work done by me and all sources listed within have been detailed in the bibliography.

Preetha Saha

(Candidate)

Dated: April 23, 2015

In my capacity as the supervisor of the candidate's project work, I certify that the above statements by the candidate are true to the best of my knowledge.

Dr. Goutam Sheet

(Supervisor)

Acknowledgement

I am thankful to my advisor Dr. Goutam Sheet for his invaluable guidance and support throughout the course of my work. I am grateful for being given an opportunity to work on the experiments which allowed me to have hands on experience on some of the most cutting edge instruments and advanced experimental techniques. I am thankful to my fellow lab mates and seniors Leena Aggarwal, Abhishek Gaurav,Jithin B.P., Shubhra Jyotsna, Shekhar Das, Mohammad Aslam, Anshu Sirohi and Ritesh Sachan for helping me during the experiments and creating an amazing and friendly lab environment to work. I extend my gratitude to Avtar Singh who works round the clock and is instrumental in keeping the lab running like a well oiled machine.

Preetha Saha

List of Figures

Contents

Abstract

Point Contact spectroscopy(PCS) is a well established and valued technique while studying electron interaction with various kinds of elementary excitations in the lattice. If the junction constriction diameter is made sufficiently small such that the transport falls under ballistic limit, electron can be given high energies(large bias across the junction) without significant heating effects (absence of scattering). These electrons at particular characteristic energies, in turn can excite the fundamental modes in the lattice structure, thus forming the basis of energy resolved spectroscopy. Consequently PCS acts as a local probe for the Fermi Surface in metals. PCS between metals and Superconductors at appropriate transport regimes gives us valuable information regarding the energy gap structure of the Superconductor. A wider scope of PCS theory allows us to determine the degree of transport spin polarization in a ferromagnet in a Superconductor-Ferromagnet point contact spectroscopy. Using a well known formalism by Blonder-Tinkham-Klapwijk for modelling Normal metal-Superconductor junctions, I have analysed the following experiments

(1) Calculating the degree of transport spin polarization in the itinerant ferromagnet CuFeSb.

(2) PCS in Pb-Ag and Pb-Co point contacts, where the differential conductance spectra suggest possibility of spin triplet pairing in mesoscopic Pb-point contacts.

Chapter 1

Introduction

1.1 Superconductivity

Superconductivity was discovered accidentally in 1911 by *Heike Kamerlingh Onnes*, one day he noticed that the resistivity of mercury dropped abruptly at $4.2K$ to a value below the resolution of his instruments. Superconductors are substances whose resistivity falls to zero below a certain temperature T_C, called the critical temperature.

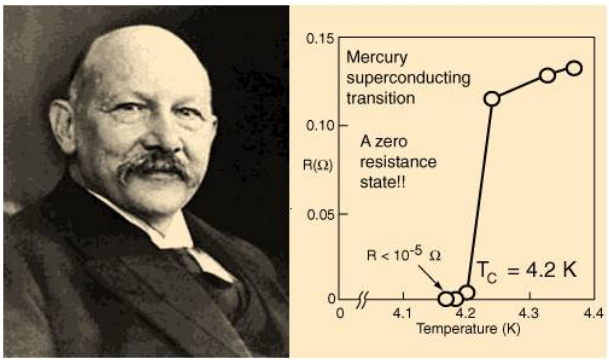

Figure 1.1: Heike Kamerlingh Onnes: Discovery of superconductivity of Mercury-1911(source:Google images)

In 1933 Meissner and Ochsenfeld discovered another property of superconductors that if

a superconductor kept in a magnetic field, is cooled below the transition(critical) temperature, the lines of the induction field B are pushed out,which means the magnetic field vanishes inside the superconductor (Meissner effect). It was shown by London(1935) that B reduces to zero inside the superconductor over a characteristic penetration depth λ nearly equal to 10^{-5} cm.

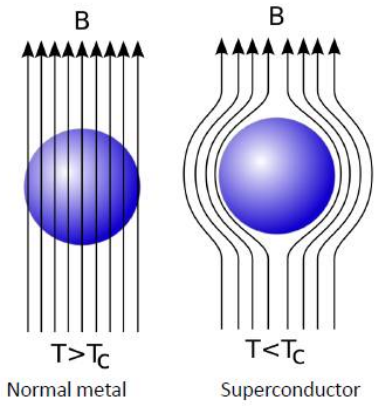

Figure 1.2: Meissner effect-Magnetic lines are pushed out of a superconductor(Source: Google images)

It has been observed that even at temperatures below the critical temperature, the application of a minimum magnetic field $H_C(T)$ [5] destroys the superconductivity.The superconductor reverts back to the normal resistance state. Critical temperature and critical magnetic field are related as follows:

$$H_C(T) = H_C(0)\left(1 - \frac{T}{T_C}\right)$$

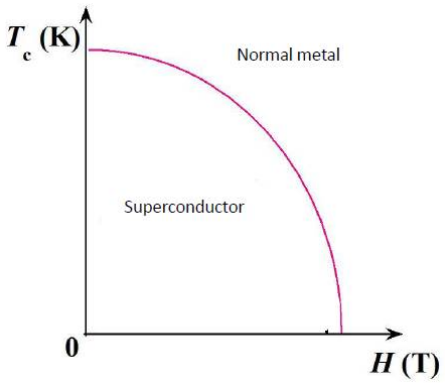

Figure 1.3: H-T phase diagram of a BCS Superconductor

Superconductors are classified into two classes Type I and Type II [1] based on their Critical Magnetic fields H_C. In Type I Superconductors, on applying an external field greater than the critical magnetic field H_C, the superconductor reverts back to the normal resistance state(Figure: 1.4 (a)) and magnetic field lines pass through the substance(H_i becomes equal to H_a).

$$H_i = H_a + \mu_0 M$$

Where $H_i$is the field inside the superconductor, H_a is the applied magnetic field and M is the magnetization of the substance(due to Meissner effect $M = -1$).

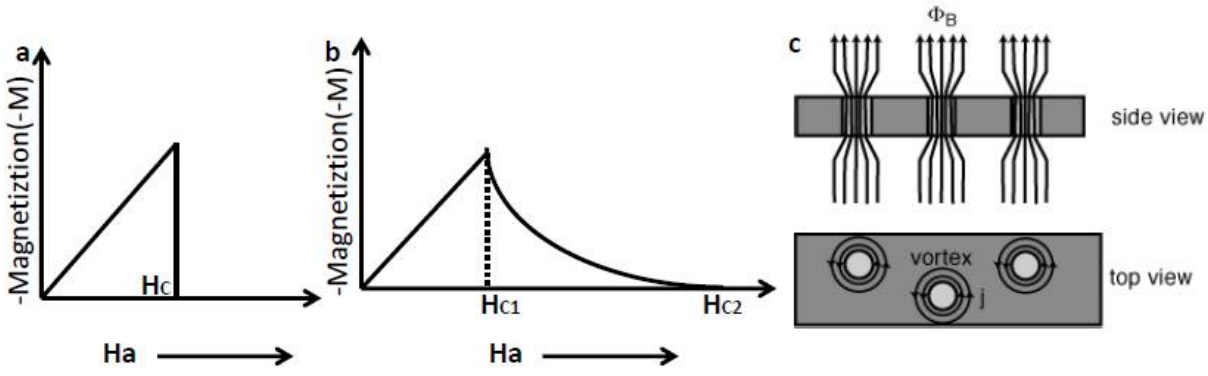

Figure 1.4: Critical Magnetic fields: (a)Type I superconductors, (b)Type II superconductors, (c)Vortices of superconducting current j at $H_{C2} > H > H_{C1}$

In Type II Superconductors there are two transitions with increasing magnetic field, at

H_{C1}, external magnetic field starts penetrating inside the superconductor (Figure: 1.4 (b)), but the entire substance doesn't revert back to the normal state. Vortices(loops of super-current)(Figure: 1.4 (c)) are created surrounding the penetrated field region(normal region). As we increase the magnetic field , the number of vortices increase, letting in more magnetic field. At H_{C2} the substance completely changes back to normal state letting in all the external magnetic field.

1.1.1 Microscopic theory of Superconductivity

The first theory regarding the inherent origin of superconductivity was given by Bardeen-Cooper-Schrieffer(BCS Theory). According to BCS theory, the interaction between electrons and phonons causes deformation of the crystal lattice such that there exists an attractive potential between the two electrons. An electron interacts with the lattice in the form of coloumbic attraction from the metallic ions. Another electron in the vicinity of the deformed lattice interacts with the lattice deformation.Therefore giving rise to an electron-electron interaction. They are said to exist in a coupled state called Cooper Pair. Theses electrons have equal and opposite momentum. At Temperature $T < T_C$ all electron undergo Bose Einstein Condensation. At $T = 0K$ in the ground state all electrons are paired and the superconducting ground state is represented as :

$$|\psi\rangle = [u_{\vec{k}} + v_{\vec{k}} c^*_{\vec{k}\uparrow} c^*_{-\vec{k}\downarrow}]|0\rangle$$

where $|0\rangle$ is the null state, $c^*_{\vec{k}\uparrow}(c^*_{-\vec{k}\downarrow})$ represents the electron operators that gives rise an electron with momenta $\vec{k}(-\vec{k})$ and spin $\uparrow$ $(\downarrow)$. While, $v^2_{\vec{k}}$ is the probability that both electrons exist in the Cooper Pair state and $u^2_{\vec{k}} = 1 - v^2_{\vec{k}}$ is the probability of vacant pair.

At $T = 0K$, the minimum amount of energy required to break the Cooper pair is called the energy gap. Order parameter defines the energy gap structure. When energy gap Δ is isotropic with k ,i.e it is symmetric in momentum space, it is said to have *S-wave symmetry* of the order parameter. The name derives its reason from the fact that net spin in the Cooper pair is zero which gives it a $S = 0$ singlet state like nature.

Unconventional Superconductors: Attractive potential between electrons can arise as a result of other interactions like magnetic interactions. For example antiferromagnetic fluctuations in high T_C cuprates [12] gives rise to a superconducting gap function in k-space that has d wave symmetry, while ferromagnetic fluctuations in Sr_2RuO_4 [11] gives rise to spin triplet pairing(p wave symmetry) of electrons.

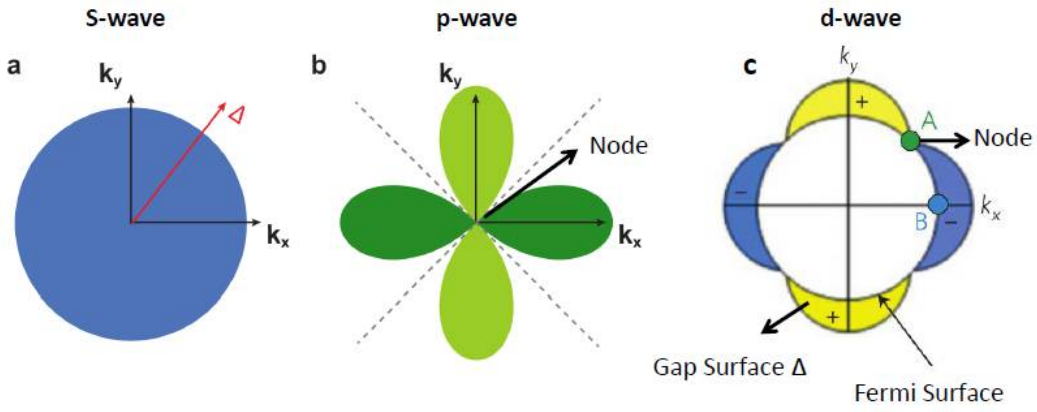

Figure 1.5: Momentum space representation of s-wave, p-wave and d-wave superconducting order parameter. Source: Google images

1.2 Point Contact Spectroscopy

A point contact is made by connecting two conductors [9] through a narrow constriction. If momentum and energy of the electron is conserved while passing through the junction, that is in the absence of scattering, it shows several interesting properties [17].

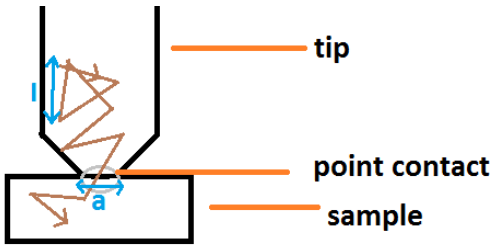

Figure 1.6: Schematic representation of a Point Contact and electron scattering while crossing the junction,'a': Cross section diameter and 'l': mean free path of the electron

1.2.1 Electron transport regimes and respective Length Scales

The conductance of a bulk conductor is given by Ohm's law:

$$G = \sigma \frac{A}{l}$$

where A and l are the area of cross-section and length of the conductor, respectively. The conductivity of the sample is determined by intrinsic material parameters, given by the *Drude* conductivity:

$$\sigma = \frac{ne^2}{2m}\tau_m$$

where n represents charge carrier concentration, τ_m is the characteristic momentum relaxation time of the charge carriers. However, Drude theory has limitations at microscopic length scales smaller than the mean free length of the electron given by $l = v_F \tau_m$, where v_F is the Fermi velocity. This length gives the distance, that the electron traverses between two successive collisions(scattering events).

Mean free length l_m is further classified as elastic mean free length $l_{elastic}$ and inelastic mean free length $l_{inelastic}$. $l_{elastic}$ corresponds to scattering cases such that energy and momentum are both preserved as in elastic collision [19]. It allows both energy and momentum resolved spectroscopy. $l_{inelastic}$ corresponds to inelastic scattering where neither energy nor momentum is conserved.

Contacts between conductors are classified based on their contact diameter 'a'. The smallest constriction diameter is limited by De-Broglie wavelength of electron [31]. A

nano-constriction [18] is in the ***ballistic regime*** if $a < l_{elastic}$, i. e. essentially no scattering occurs inside the conductor. On the contrary, for conductors in the **thermal regime** ($a > l_{inelastic}$) due to scattering energy resolved spectroscopy is difficult. Constriction with diameter in the range $l_{inelastic} > a > l_{elastic}$ are defined to be in the intermediate or ***Diffusive regime*** In such a regime energy is conserved.

Resistance in the ballistic regime is given by *Sharvin's* Formula (Sharvin 1965):

$$G_S = \frac{2e^2}{h}\left(\frac{k_F a}{2}\right)^2$$

where, $'a'$ is the junction diameter and $'k'_F$ represents the Fermi wave vector. Resistance of constrictions in the thermal regime is same as that calculated in the bulk material. For junction diameters in the diffusive regime, approximation for resistance is given the Wexler's equation [32]

$$R_W = \Gamma\frac{\rho(T)}{2a} + \frac{2\hbar/e^2}{(ak_F)^2}$$

it can be decomposed as the sum of the resistances obtained in the thermal and ballistic regime.

If the junction constriction diameter is made sufficiently small such the transport falls under ballistic limit, electron can be given high energies(large bias across the junction) without significant heating effects (absence of scattering). These electrons at particular characteristic energies in turn can excite the fundamental modes in the lattice structure, thus forming the basis of energy resolved spectroscopy [8]. Therefore point contact spectroscopy can act as a localized probe for the Fermi surface.

1.2.2 Andreev reflection

Point Contact Spectroscopy of Normal Metal-Superconductor ($N - S$) junctions are mainly used to measure the energy gap of the involved superconductor [6],[10]. Using this information lower bounds of Fermi velocity and coherence length of the superconductor can be calculated.

In $N - S$ junction transport measurement, as current(electrons) is passed through the junction, three processes can occur at the interface: (1) Transmission, (2) Reflection and (3) Andreev reflection. The respective probabilities of occurrence of each process depends on the size of the junction and barrier potential. The potential of the junction is characterised by the dimensionless parameter Z such that a negligible barrier(transparent) easy to pass is given by $Z = 0$, while a large potential that stops electrons is given by $Z > 1$.

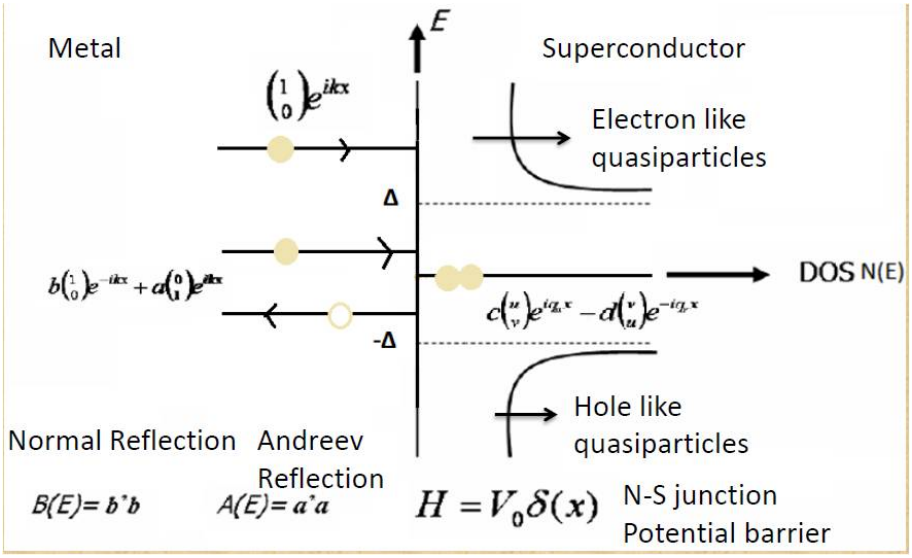

Figure 1.7: Schematic representation of N-S junction showing energy versus density of states on each side

At temperatures below the critical temperature of the superconductor ($T < T_C$). There is a gap in density of states that opens up at energy Δ. According to BCS theory, at $T = 0K$, in the absence of thermal agitations, electrons exist in the form of Cooper Pair. At appropriately low temperatures, it is thermodynamically more favourable for electrons of opposite spin to bind together(Cooper Pair). Cooper pairs break and form quasiparitcles, for energies above the gap. Therefore the energy gap is also called the binding energy. There are no quasiparticle states available at energies $E < \Delta$.

Travelling from the metal, if the incident electron at the junction possesses energy greater than Δ, due to availability of quasiparticle states in the superconductor(at $E > \Delta$), it gets

transmitted across the interface. Here electrons from normal metal flow through the junction into the superconductor and shows constant differential conductance(characteristics of linear I-V spectra).

For electron with energies between the gap ($E < \Delta$), the differential conductance depends on the cross section of the junction and potential of the junction barrier Z. In case of point contacts with a large cross section(thermal regime transport), it is seen that irrespective of the value of Z, the electron cannot pass across the junction and gets reflected from the interface back into the metal, hence differential conductance ($\frac{dI}{dV}$) is zero in this regime. At exactly the gap energy Δ there is a discontinuity in I-V curve which manifests itself as sharp peak in the $\frac{dI}{dV}$ characteristics. Width of this peak is temperature dependent as thermal fluctuations leads to broadening that destroys the Cooper pairs.

If the constriction cross section is in the ballistic regime, for small junction potential Z with electron energy $E < \Delta$ a phenomenon called Andreev reflection occurs and differential conductance increases by a factor of two as compared to the conductance at energies above the gap (Figure 1.8 (a)). Physically we can analyse the process as follows, for an electron with $E < \Delta$ to cross the junction and enter inside the superconductor, it can only exist in the form of Cooper pair, therefore it binds with an electron of opposite spin inside the superconductor. As a result, a hole - a mathematical construction to explain the imbalance of charge created in the absence of an electron, is reflected back into the normal metal with exactly opposite spin and momentum of that of the incident electron. Therefore if the incident electron possesses current density ev_F, then current $-(-ev_F)$ is reflected as hole. As a result we have current of $2ev_F$ in the normal metal and $2ev_F$ in the superconductor due to the Cooper pair.

In a real $N-S$ junction the barrier potential will be finite and hence increase in differential conductivity for $E < \Delta$ will be less than twice Figure 1.8. For large valus of barrier potential Z, the transport regime falls under tunnelling regime. The current is zero below ($E < \Delta$) and At exactly the gap energy Δ there is a discontinuity in I-V curve which manifests itself as sharp peak in the $\frac{dI}{dV}$ characteristics.

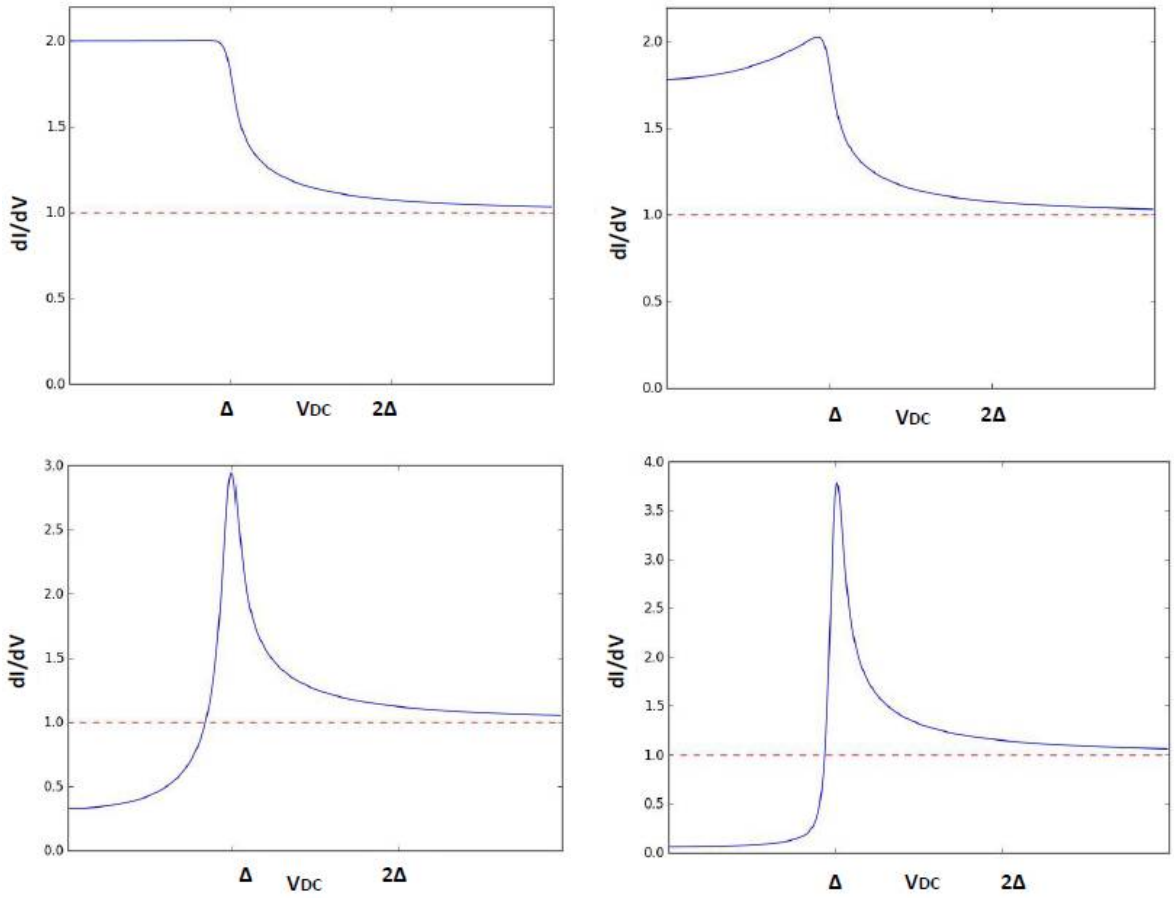

Figure 1.8: Z dependenc of Differential Conductance$\frac{dI}{dV}$ plots with respect to V_{DC}(potial across junction): (a)$Z = 0.02$ nearly trasparent barrier, (b)$Z = 0.2$ $\frac{dI}{dV}$ less than exactly twice in $E < \Delta$ region,(C)$Z = 1.2$ $\frac{dI}{dV}$ going towards zero, (d)$Z = 3$ At very high value of Z, $\frac{dI}{dV}$ is zero in the $E < \Delta$ region.

1.2.3 BTK Model

The theory used to model [6] the point contact electron transport across the junction considers transmission, reflection and Andreev reflection. Junction barrier potential is taken as δ-function barrier of amplitude H. Incident wave is considered one dimensional plane wave travelling from normal metal into the superconductor. This one dimensional model is based for superconductors with energy gap symmetric in momentum space i.e. BCS superconductors(s-wave superconductor).

Solution of the BTK Model[10] The following section has been written with help from [10] To find the probabilities of the respective processes of transmission, reflection and Andreev reflection, we have to solve *Bogoliubov-de Gennes equations(BdG)*

$$\phi = (f(x,t), g(x,t))$$

where f(x,t),g(x,t) are electron and hole wave functions respectively. The BdG equation is as follows:

$$i\left(\hbar\frac{\delta}{\delta t} + \Gamma\Theta(x)\right)\sigma_z\phi = \left(-\frac{\hbar^2}{2m}\frac{\delta^2}{\delta x^2} - \mu(x) + V(x)\right)\sigma_z\phi + \Delta(x)\sigma_x\phi$$

where σ_x, σ_z are Pauli matrices, $\Theta(x)$ is the step function such that it is zero for negative values of x, while unity for x equal to zero and positive values of x, $V(x)$ is the potential energy, $\mu(x)$ is the chemical potential and $\Delta(x)$ represents the energy gap. The rate at which the quasi particles decay to the BCS ground state is represented by parameter Γ. Say τ is the lifetime of these particles, then

$$\Gamma = \frac{\hbar}{\tau}$$

The parameter Γ accounts for the quasi particle decay through scattering. It broadens the peak as shown in figure. μ is the energy required to add particles to the system. The barrier potential is characterized by a dimensional parameter Z,

$$Z = \frac{H}{\hbar v_{FS}}$$

where v_{FS} is the fermi velocity in the superconductor.

The plane wave equations at the N-S junctions are as follows:

$$\psi_i = \begin{pmatrix} 1 \\ 0 \end{pmatrix} \mathrm{e}^{\mathrm{iq^+x}} \mathrm{e}^{-\mathrm{iEt}/\hbar}$$

$$\psi_r = \left[a \begin{pmatrix} 0 \\ 1 \end{pmatrix} \mathrm{e}^{\mathrm{iq^-x}} + \mathrm{b} \begin{pmatrix} 1 \\ 0 \end{pmatrix} \mathrm{e}^{-\mathrm{iq^+x}} \right] \mathrm{e}^{-\mathrm{iEt}/\hbar}$$

$$\psi_t = \left[c \begin{pmatrix} u_0 \\ v_0 \end{pmatrix} \mathrm{e}^{\mathrm{ik^+x}} + \mathrm{d} \begin{pmatrix} v_0 \\ u_0 \end{pmatrix} \mathrm{e}^{-\mathrm{ik^-x}} \right] \mathrm{e}^{-\mathrm{i(E+i\Gamma)t/\hbar}}$$

where ψ_i,ψ_r,ψ_t, represent the incident, reflected and transmitted wave functions respectively. The wave vectors in the metal and superconductor and q and k respectively. Also inside the superconductor the electron and hole are not independent fermions but rather quasiparticles. As a result their eigen vectors differ from electron/hole states and have both non-zero components u_0 and v_0. The boundary values are:

Continuity of wave functions at the junction

$$\Psi_N(0) = \Psi_S(0)$$

where $\Psi_N = \psi_t + \psi_r$ and $\Psi_S = \psi_t$ and discontinuity of the first derivative across the δ-function.

$$-\frac{\hbar^2}{2m}\left(\frac{d\Psi_S(0)}{dx} - \frac{d\Psi_N(0)}{dx}\right) + H\Psi_S(0) = 0$$

Using these equations we get the values of $q^{+/-}$ and $k^{+/-}$ and

$$u_0^2 = 1 - v_0^2 = \frac{1}{2}\left[1 + \frac{\sqrt{E^2 - \Delta^2}}{E}\right]$$

Solving the given equations we get the probabilities for Andreev reflection A and normal reflection B as:

for $E < \Delta$:

$$A(E) = \frac{\Delta^2}{E^2 + (\Delta^2 - E^2)(1 + 2Z^2)^2}$$

$$B(E) = 1 - A$$

for $E > \Delta$:

$$A(E) = \frac{u_0^2 v_0^2}{\gamma^2}$$

$$B(E) = \frac{(u_0^2 - v_0^2)^2 Z^2 (1 + Z^2)}{\gamma^2}$$

Simulations of the BTK Model:

Varying the value of energy gap Δ: As shown in figure 1.9 the peaks close to V=0 are the signature features of Andreev reflection

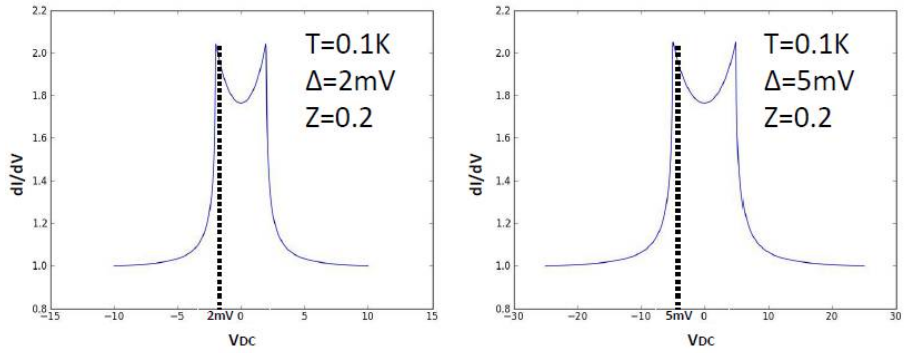

Figure 1.9: Changing value of Δ changes the position of the Andreev peaks

Varying the value of Barrier potential Z, keeping Temperature and Δ constant.

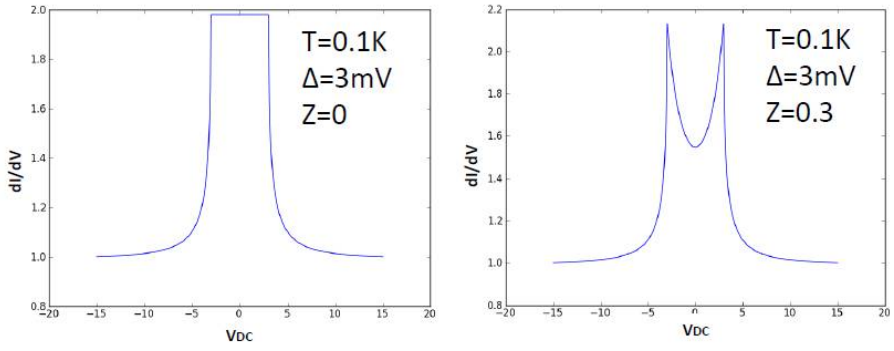

Figure 1.10: Increase in Z causes $\frac{dI}{dV}$ to reduce in $E < \Delta$ region

Varying Temperature:

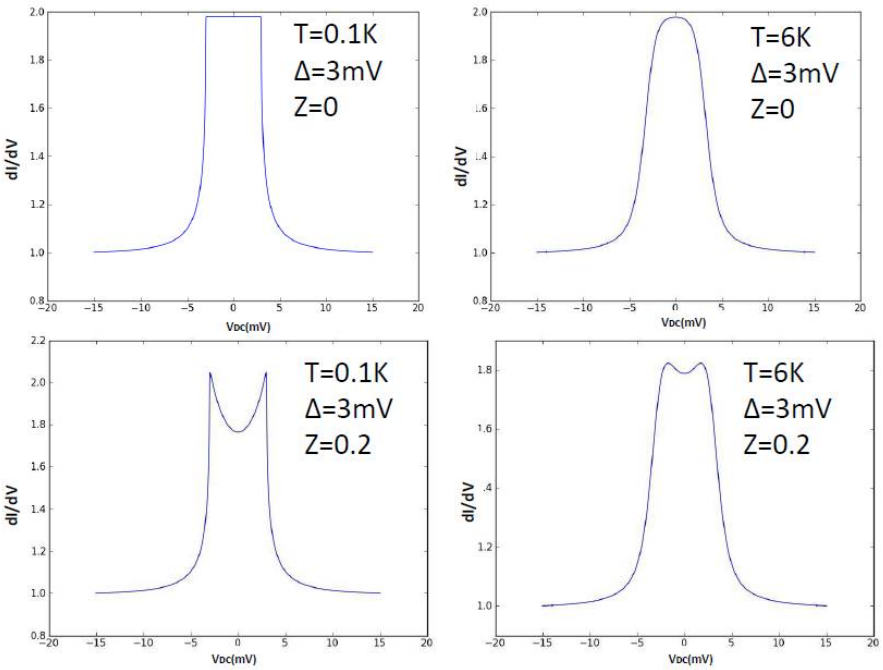

Figure 1.11: Increase in Temperature causes broadening of the Andreev features

Current across the junction [10] The probability of tunnelling across the junction is the product of number of initial occupied states and the final number of unoccupied states. For tunnelling across normal metal to the superconductor, number of occupied initial states is $N_N(E)f(E)$ and number of final unoccupied states is $N_S(E+eV)[1-f(E+eV)]$. Here $N_N(E)$ and $N_S(E)$ are density of states of the metal and superconductor respectively and $f(E)$ is the Fermi function. For current in the opposite direction net probability equals $N_N(E)f(E+eV)N_S(E+eV)[1-f(E)]$ Subtracting reverse current from the forward current we get the net current I_{NS} as :

$$I_{NS} \propto \int_{-\infty}^{\infty} N_N(E)f(E+eV)[f(E)-f(E+eV)]dE$$

Using BTK Model to include the effect of Andreev reflection, the current flow across the junction is

$$I_{NS} \propto \int_{-\infty}^{\infty} (1+A(E)-B(E))f(E)-f(E+eV)dE$$

Here $1+A(E)-B(E)$ is the transmission coefficient such that when a hole is reflected, a positive charge moves in the opposite direction of the incident electron and thus adds

to the current. It is represented by A(E). Simply reflected electron represented by B(E) reduces the current

1.2.4 Spectral broadening

The BTK Model simulates electronic transport through Normal metal/Superconductor junctions considering ballistic regime of transport. Although this theoretical model quite accurately agrees with the experimental results, there have been a number of cases where the discrepancy between the experimental data and theoretical fit is significant. Most of such experimental spectra show broadening effects and decrease in differential conductance. It is therefore required to consider the possibility of inelastic scattering at the junction. This leads to shortening of quasiparticle lifetime τ. Spin fluctuation also leads to broadening of the gap structure(Andreev feature). This effect has been incorporated in the existing BTK Model [21], such that new expression for Probabilities of Andreev reflection A(E) and normal reflection B(E) have an additional complex term Γ added to the energy.

$$\Gamma = \frac{\hbar}{\tau}$$

This can be interpreted as decrease in energy due to the inelastic scattering. Increasing the value of Γ has smearing effects on the differential conductance peaks.

Modified coherence factors u_0 and v_0 become:

$$u_0^2 = 1 - v_0^2 = \frac{1}{2}\left[1 + \frac{\sqrt{(E+i\Gamma)^2 - \Delta^2}}{E+i\Gamma}\right]$$

and in turn the probabilities of Andreev and normal reflection $A(E) and B(E)$ become:

$$A(E) = \frac{\sqrt{(\alpha^2+\eta^2)(\beta^2+\eta^2)}}{\gamma^2}$$

$$B(E) = Z^2\frac{[(\alpha-\beta)Z - 2\eta]^2 + [2\eta Z + (\alpha-\beta)]^2}{\gamma^2}$$

where $u_0^2 = \alpha + i\eta$ and $v_0^2 = \beta - i\eta$

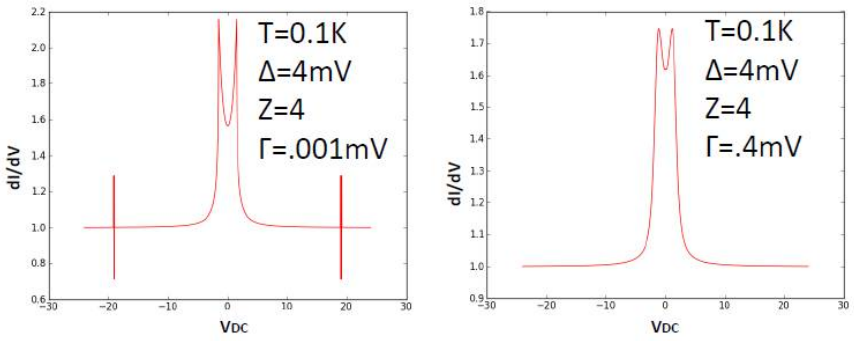

Figure 1.12: Effect of parameter Γ which increases with decrease in quasiparticle lifetime τ. $\frac{dI}{dV}$ decreasing and broadening with increase in Γ.

1.2.5 Spin Resolved Point Contact Spectroscopy

In ferromagnets there is a discrepancy in the density of states of spin up and spin down band electrons. Classically in solid states, spin polarization is P is defines as the ratio of difference in the number density of electrons of spin up and spin down band with respect to the total density of states.

$$P = \frac{N\uparrow - N\downarrow}{N\uparrow + N\downarrow}$$

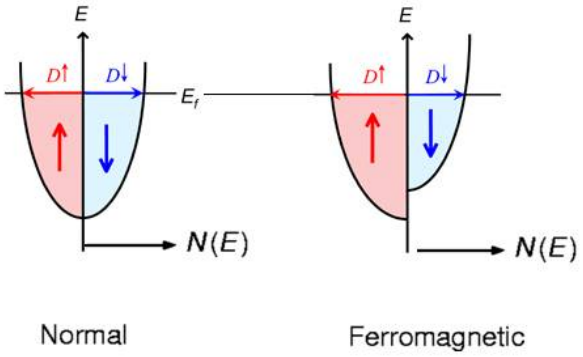

Figure 1.13: Density of states in normal metal and ferromagnets.

However while studying electron transport through ferromagnet-metal junctionsc[14], we

cannot directly measure the density of states and thus classical definition cannot be used to support the experimental data. A modified definition of spin polarization [14] given by Bloch-Boltzmann transport theory in terms of current densities J in the spin up band and spin down band gives us transport spin polarization P_t such that,

$$P_t = \frac{J\uparrow - J\downarrow}{J\uparrow + J\downarrow}$$

Current density J depends of the Fermi velocity v_F. The nature of dependence in turn is dependent on the transport regime. The ballistic and diffusive limit have the following definitions of J respectively,

$$J\uparrow_{ballistic} = \langle N\uparrow v_F\uparrow\rangle$$

and

$$J\uparrow_{diffusive} = \langle N\uparrow v_F^2\uparrow\rangle$$

As we consider Andreev reflection across the Superconductor-ferromagnet junction [26], it is evident from the discrepancy in the density of states of the spin up and down down bands in ferromagnet, that corresponding to the theory of Andreev reflection, not all incident electrons(of any particular band, say spin up) will have a reflecting hole from the opposite spin band. As a result increase in differential conductance in the energy gap region is suppressed as compared to that in normal metal - superconductor junctions.

A new model that takes into effect the amount of transport spin polarization in a ferromagnet and gives the corresponding Andreev reflection probability is as follows:

Net current through the junction is a combination of I_U and I_P, where I_U corresponds to the current without any spin polarization and I_P correspond to the current using 100% spin polarization, which has separate Andreev reflection and normal reflection coefficients $A_P(E)$ and $B_P(E)$ respectively, given by:

$$A_P(E) = 0$$

$$B_P(E) = \frac{(1-\sqrt{\epsilon)^2} + 4Z^2\epsilon}{(1+\sqrt{\epsilon)^2} + 4Z^2\epsilon}$$

where $u_0^2 = \frac{1}{2}(1 + \sqrt{\epsilon})$, $\epsilon = \frac{E^2 - \Delta^2}{E^2}$ and Z is the barrier potential.

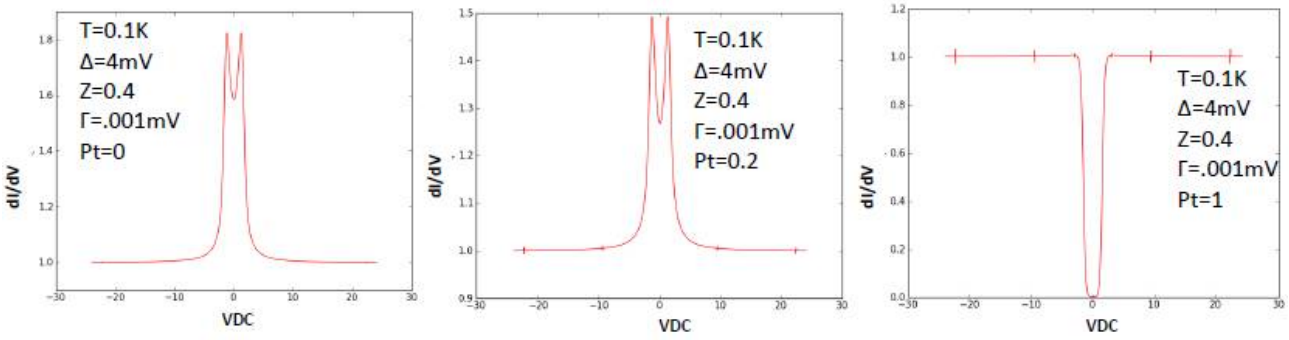

Figure 1.14: Dependence of diferential conductance on degree of transport spin polarization P_t of the sample

Then the current for an intermediate spin polarization P_t is calculated by interpolation between I_U and I_P following the relation given by:

$$I_t = I_U(1 - P_t) + I_P P_t$$

The derivative of I_t with respect to V gives the modified Andreev reflection spectrum with finite spin polarization.

1.2.6 Role of Critical Current:

If a point contact falls under diffusive or thermal regime, We see certain sharp peaks in the differential resistance spectra as in figure 1.15 (b). These sharp peak arise as a result of sudden non linearities in the I-V spectrum [25]. The point contacts not being in the completely ballistic regime are prone to scattering effects(finite normal state resistance), as soon as the critical current of the point contact is reached while sweeping the current, superconductivity is destroyed and the point contact has a finite resistance. This sudden change in I-V spectrum manifest themselves as sharp peaks in the $\frac{dV}{dI}$ spectra. The peaks are hence called the critical current peaks.

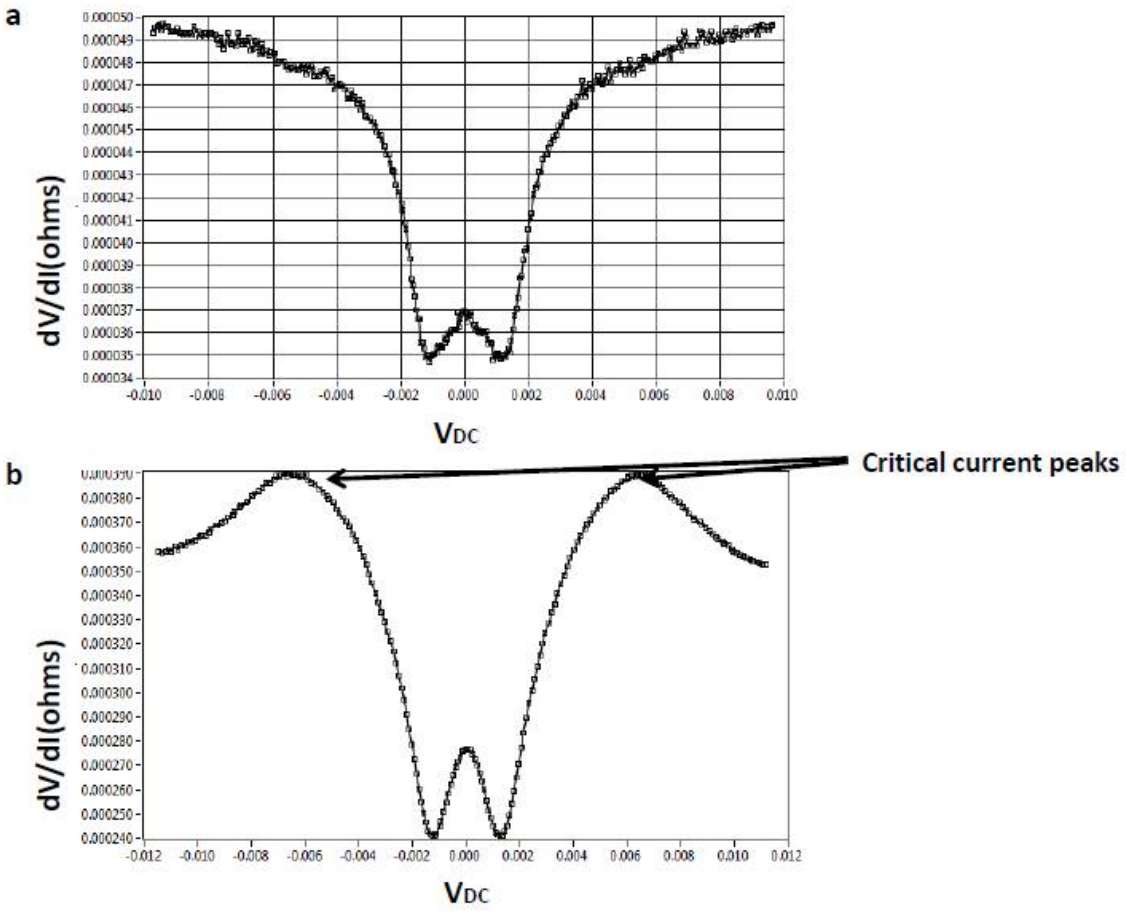

Figure 1.15: (a) $\frac{dV}{dI}$ spectra in compltely ballistic regime. (b)$\frac{dV}{dI}$ spectra showing Critical current peaks in non ballistic regime point contacts

The critical current peaks can arise at any value of V_{DC} depending on the critical current of that particular point contact. Figure 1.15 shows a comparison between the Andreev spectra of two point contacts one in completely ballistic regime(resistance resistance doesn't change even after critical current is reached)and another showing critical current peaks of the point contact in diffusive regime.

In the following figure 1.16 we see a summary of Pb-Ag point contacts in Ballistic, Thermal and Diffusive(Intermediate) regimes.

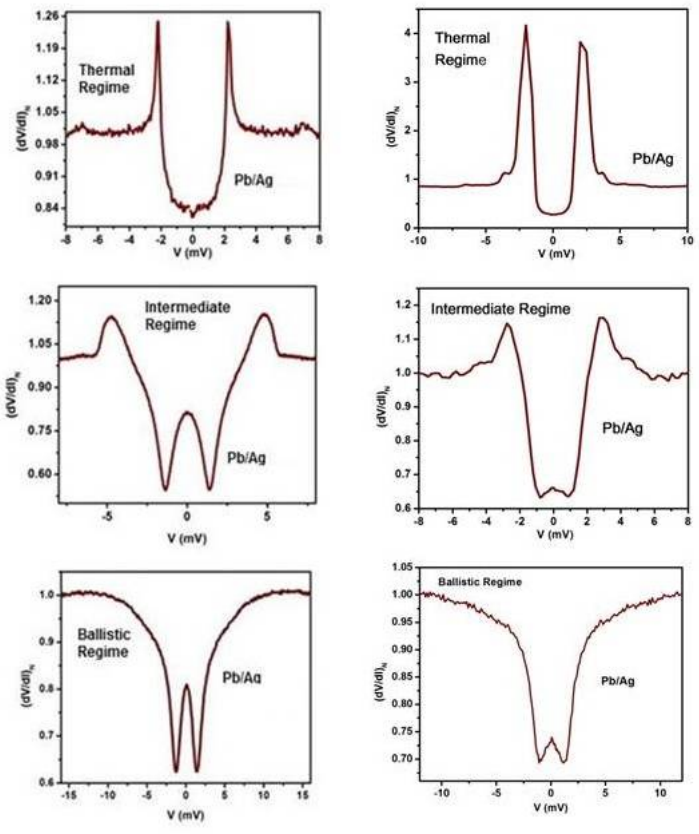

Figure 1.16: Summary of dV/dI spectra in Thermal, Intermediate(Diffusive) and Ballistic regimes

1.2.7 Experimental Setup

Andreev reflection spectroscopy experiments include the following setup and their corresponding data acquisitions techniques.

1.Point Contact fabrication:

In our experiments we employed "Needle Anvil" method to form the Nano constrictions [17]. A sharp tip(Superconductor/Metal) is brought into contact with a flat surface(Metal/Superconductor) using a differential screw, thus forming a transport pathway of a very small diameter. The resulting point contact acts as a local probe to study the Fermi surface properties of the sample.

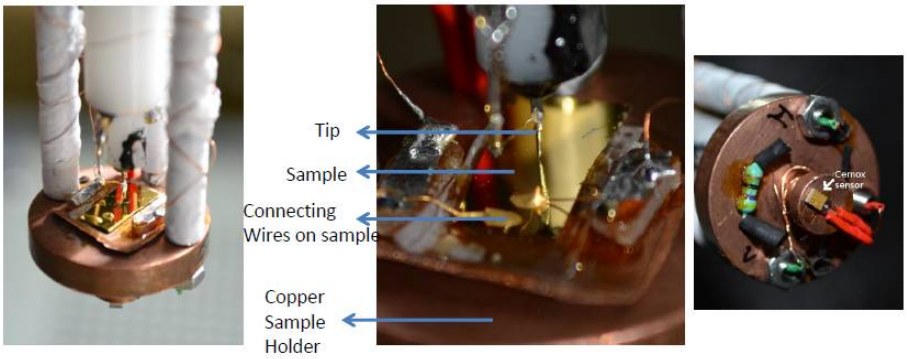

Figure 1.17: Sample holding space of the probe, cernox thermometer-temperature sensor

2. Differential conductivity with respect to electron energy

Differential Conductance:

As the electrons pass through the junction non linearities arising in the Current(I) as a function of Voltage(V) greatly manifest themselves when plotted in the form of dI/dV called Differential Conductance. Electron energy is proportional with respect to Voltage difference across the junction. dI/dV can be obtained by either of the following ways:

(1) A current Voltage sweep and then the derivative : A relatively easy method to setup, requiring one source and one voltage measuring instrument. This method has various drawbacks, even a small noise in the I-V spectrum becomes a large noise when the measurements are differentiated. Also large current can cause significant joule heating.

(2)AC lock-in modulation technique of applying very small sinusoidal signal ($I_{AC}cos(\omega t)$) superimposed over a DC bias across the junction and using the lock-in again to read the AC current and AC Voltage drop across the junction. Writing the voltage expression in the form of Taylor Series,

$$V(I_{DC} + I_{AC}cos(\omega t)) = V(I_{DC}) + \frac{dV(I_{DC})}{dI} I_{AC}cos(\omega t) + ...$$

This clearly indicates that measuring the AC Voltage gives dV/dI. We have used this technique for our measurements of Andreev reflection spectrum. dI is proportional to the excitation current set during the experiment. The data acquisition was done by using a

labview programme developed in house.

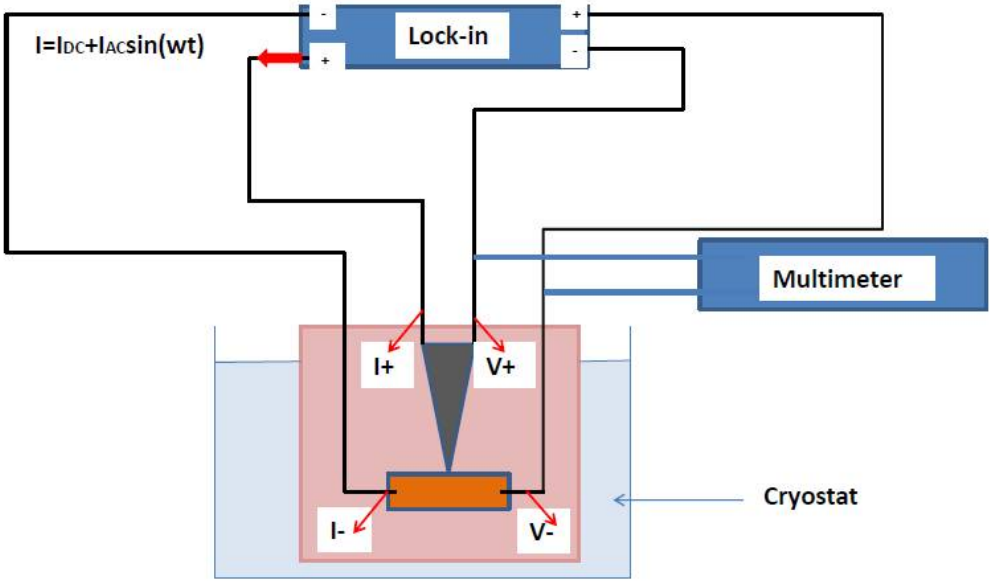

Figure 1.18: Schematic dscription of the measurement setup

The instruments used for the measurements are KEITHLEY2000 Multimeter for measuring the DC Voltage, SRS 830 Lock-in Amplifier, Lakeshore350 for measuring the temperature of the sample inside the cryostat.

Chapter 2

Spin-resolved Point Contact Spectroscopy on CuFeSb

Spectroscopic evidence of high transport spin-polarization in ferromagnetic CuFeSb

Preetha Saha[1], *Abhishek Gaurav*[1], *Shubhra Jyotsna*[1], *Gohil S. Thakur*[2], *Zeba Haque*[2], *L. C. Gupta*[2], *Ashok K. Ganguli*[2,3], *and Goutam Sheet*[1]

[1]*Department of Physical Sciences, Indian Institute of Science Education and Research Mohali,*[2]*Department of Chemistry, Indian Institute of Technology, New Delhi,*[3]*Institute of Nano Science and Technology, Mohali*

Introduction:

Transport Spin Polarization of the itinerant ferromagnet CuFeSb was measured using spin-resolved Andreev reflection spectroscopy. The spectra were analysed using a modified Blonder-Tinkham-Klapwijk (BTK) formalism that includes Fermi-level spin polarization and spectral broadening due to finite quasiparticle lifetime. We found that the intrinsic transport spin polarization in CuFeSb is approximately 50%. This is significantly different from the half metallic behaviour of CuFeSb as expected from band-structure cal-

culation. We attribute this difference to possible difference in the Fermi velocities in the spin up and the spin down bands of CuFeSb.

Theory:

It is believed that the exotic superconductivity in the iron-based pnictide and chalcogenide superconductors originates from a magnetically driven pairing mechanism where the superconducting order is thought to be coupled with spin fluctuations [2]. Therefore, in order to understand the nature of coupling between the superconducting order and spin fluctuations, it is imperative to understand the nature of magnetism and the spin fluctuations in the parent compounds from which the superconducting states are derived through doping.

Recently it has been shown that CuFeSb [22], which is isostructural to the iron-based layered superconductors e.g., Li(Na)FeAs, has a ferromagnetic ground state [23]. A close relative of this compound CuFeAs [30] stabilizes in an antiferromagnetic ground state. The ferromagnetic order in CuFeSb is thought to originate from the large height of Sb from the Fe plane. This fact also supports the hypothesis that the competing magnetic interactions in ferropnictide superconductors is decided by the anion height i.e., there is a gradual change in the magnetic properties from superconductivity to antiferromagnetism to ferromagnetism on moving in the increasing order of anion height from LiFeAs to CuFeAs to CuFeSb [15].

CuFeSb has been known to be the only material in the FeAs or FeSb family that shows a ferromagnetic ground state. Therefore it is most important to understand the Fermi surface properties of this unique system by spectroscopic measurements, in particular, the nature of the Fermi surface spin polarization.

Experiment:

Here we have employed spin-resolved Andreev reflection spectroscopy [26] using conventional superconducting tips to measure the transport spin polarization P_t at the Fermi level of CuFeSb. From the analysis of the Andreev reflection data between the super-

conductor and the ferromagnet [29], we found the evidence of a high degree of transport spin polarization approaching 50% in CuFeSb. This fact is of important consequence as ferromagnets with more than 50% transport spin polarization are potential candidates as spin source in spintronic devices.

As discussed in the introduction, transport through a ballistic point contact between a normal metal and a superconductor is dominated by Andreev reflection that involves the reflection of a spin up(down) electron as a spin down(up) hole from the interface [6] . The Andreev reflection spectra can be fitted using two fitting parameters,Z and Δ. However, in the system where the life-time of the quasiparticles is finite due to inelastic processes at the interface and spin fluctuation [16], the Andreev reflection spectrum undergoes broadening. Such spectra are analysed by a modified BTK formalism using three parameters Z, Δ and Γ.

In a superconductor-ferromagnet junction as in this case, we expect the Fermi level to be spin polarized [28], as a result increase in differential conductance(below $E < \Delta$) is suppressed depending on the amount of spin polarization. Accordingly the analysis and fitting of such spectra is done using a further modified BTK Model [27] that takes into account the spin polarized Fermi surface. Thus the parameters required for fitting are Z, Δ, Γ and P_t.

It should be noted that for the measurement of the spin polarization of ferromagnets standard conventional superconducting probes are used for which the value of Δ is known. In addition, in order to have superconductivity, Γ cannot be arbitrarily large with respect to Δ. Therefore, effectively only two parameters, Z and P_t, are tuned freely during the analysis of spin-polarized Andreev reflection spectra. For fitting the experimental data theoretical spectra were generated by a code written in python.

The measurements were performed on a polycrystalline pellet of CuFeSb and superconducting tip Nb and Pb were used. CuFeSb shows a ferromagnetic transition around 380 K. The Andreev reflection spectroscopic measurements were performed by measuring the transport characteristics of several ballistic point-contacts between CuFeSb and the

elemental superconductors niobium (Nb) and lead (Pb) respectively using a home-built point-contact spectroscopy probe in a liquid helium cryostat.

A calibrated cernox thermometer and a heater were attached to the same copper disc for precise measurement of the temperature and for controlling the sample temperature. Two $100\mu m$ thick gold wires were mounted on the sample for transport measurements. The superconducting tips were fabricated from $250\mu m$ diameter wires of Nb and Pb respectively. The tips were mounted on a teflon piece connected to the head of a 100 threads per inch differential screw. Two more $100\mu m$ thick gold wires were mounted on the tip. The probe was then mounted inside the static variable temperature insert (VTI) of a liquid-helium cryostat. The static VTI was surrounded by a dynamic VTI with a micro-capillary that allowed us to perform measurements down to $1.4K$.

In figure 2.1 we see Andreev reflection spectra between Nb and CuFeSb. The spectra clearly show the double-peak structure symmetric about $V = 0$, which is the hallmark of Andreev reflection. For low values of Z, these peaks appear close to the energy gap of the superconductor. The solid lines show the theoretical fits as per the model described above. The superconducting energy gap of niobium is found to be approximately between $1meV$ and $1.5meV$ for all the point contacts that we have analysed, indicating the proximity of the ferromagnet does not suppress the superconductivity of the point-contacts significantly.

The value of Γ remained zero for all the spectra, which means the broadening due to finite quasiparticle lifetime is absent at the point-contact. This fact also indicates that the spin fluctuation in the system is not significant as strong spin fluctuations is also known to give rise to large Γ.

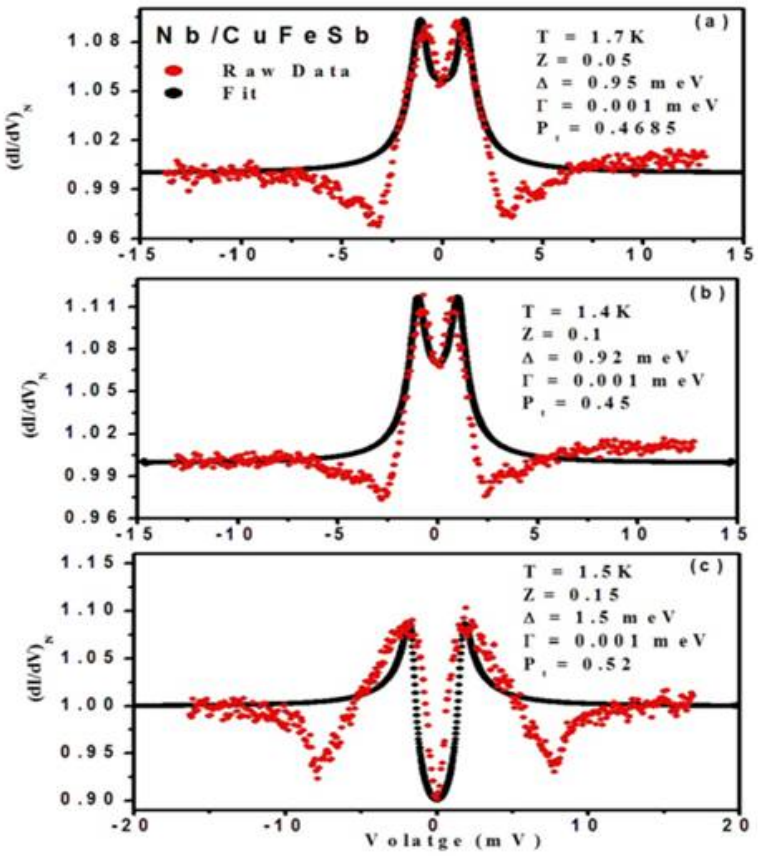

Figure 2.1: Fitting of Andreev reflection spectra of CuFeSb with Niobium

It is found that the raw data deviate slightly from the fit at certain points (notice the dip structures in dI/dV). Such deviation is known to originate from the critical current of the superconductor when a small part of the Maxwell's resistance is also measured along with the Sharvin resistance in the point-contacts close to the ballistic regime.

On repeating the experiment with Pb tip, figure 2.2 spectra were found to be considerably broader than the theoretically generated spectra. This can be attributed to the low-energy phonon modes of Pb that couple strongly with the quasiparticles and might modify the point-contact spectra. However, the low-energy part of the spectra clearly show the signature of Andreev reflection (the double-peak structure symmetric about $V = 0$). Spectra near $V = 0$ fitted nicely and the relevant parameters were extracted by fitting the low-bias portion of the spectra. Again, in such fittings, the value of Γ remained

almost zero and the superconducting energy gap was found to be approximately $1meV$ which is same as the superconducting energy gap of bulk Pb.

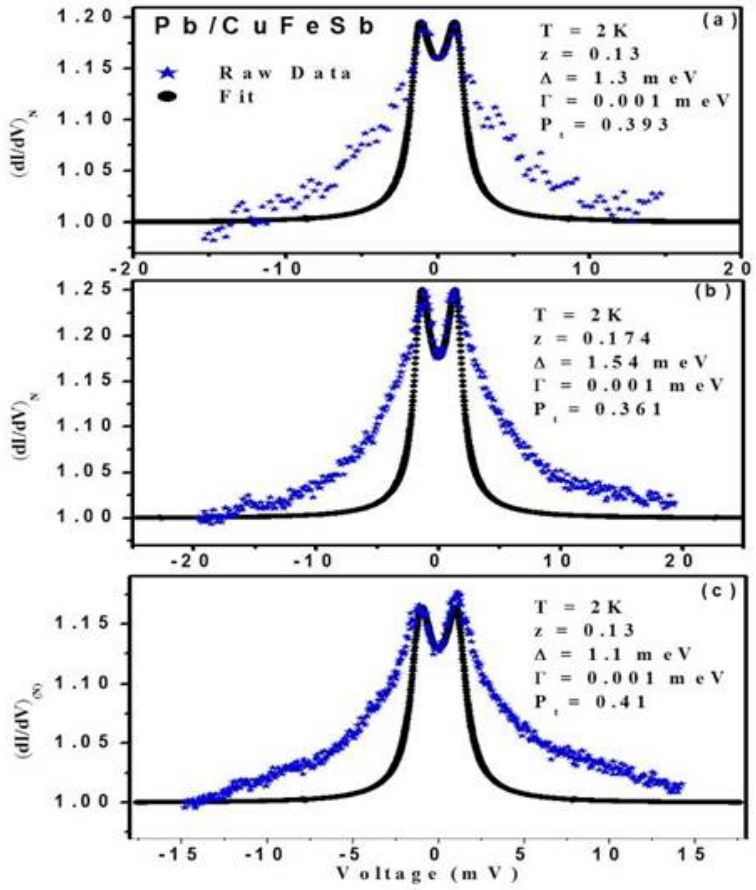

Figure 2.2: Fitting of Andreev reflection spectra of CuFeSb with Lead

On plotting a curve of P_t with respect to the Z value figure 2.3, for both Nb and Pb spectra, we observe that for most of the Nb/CuFeSb point-contacts, the value of Z was found to be small (< 0.2) For such point-contacts, the maximum measured value of P_t is found to be 52%. For the Nb/CuFeSb, Pt did not change noticeably with Z. It should be noted that within the BTK formalism, no correlation between Pt and Z is expected. For the Pb/CuFeSb point contacts, however, Pt shows small dependence on Z and the dependence is linear. The measured value of P_t decreases with increasing strength of the barrier (represented by Z).

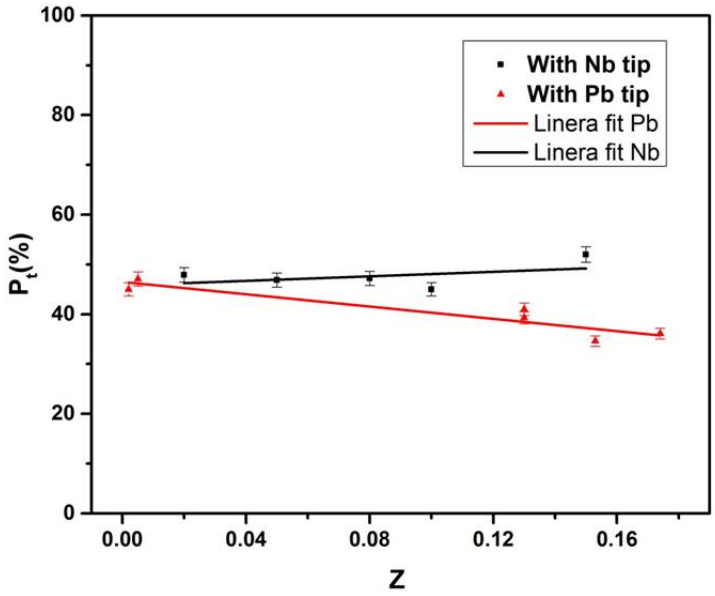

Figure 2.3: Z dependence of transport spin polarization P_t for CuFeSb-Nb and CuFeSb-Pb spectra, Though Pt shows different dependence on Z, the intrinsic value of Pt extracted for $Z = 0$ is identical for both Nb and Pb tips.

The observed dependence of P_t on Z is not understood in the BTK formalism. In such cases the dependence is attributed to spin depolarization at a magnetically disordered scattering barrier formed at the interface. In such cases, the conventional way of finding the intrinsic transport spin polarization is to extrapolate the P_t vs Z curve to Z = 0. By doing this extrapolation, the intrinsic Pt is found to be approximately 47% which is nearly equal to the value measured with the Nb tip. Therefore, it is rational to conclude that the degree of spin polarization at the Fermi level of CuFeSb is approximately 50%.

The accurate value of the transport spin polarization can be obtained only from the point-contacts that are in the ballistic or diffusive limit of transport. For our analysis, we have carefully chosen only the spectra that show the double-peak structure symmetric about $V = 0$, which is a clear signature of Andreev reflection in the ballistic or diffusive limit.

Some of the spectra we have presented here show very small conductance dips indicating that the point-contacts were close to the ballistic limit containing negligibly small contribution of thermal resistance.

The experimentally obtained value of the intrinsic spin-polarization at the Fermi level is significantly different from the spin-polarization estimated by local spin density calculations earlier performed by Sargolzaei [24]. According to this calculation, the Fermi-level is almost 100% spin polarized that makes CuFeSb a half-metallic ferromagnet.

The significant amount of discrepancy could be explained as follows,

In our experiments we measure current densities $J\uparrow$ and $J\downarrow$. Accordingly the appropriate definition of Transport spin polarization is

$$P_t = \frac{J\uparrow - J\downarrow}{J\uparrow + J\downarrow}$$

Taking into account the definitions of the current density J in both ballistic and diffusive limit,$J\uparrow_{ballistic} = \langle N\uparrow v_F\uparrow\rangle$ and $J\uparrow_{diffusive} = \langle N\uparrow v_F^2\uparrow\rangle$, we can see it always depends on the Fermi velocity. Therefore even if according to the classical definition $P = \frac{N\uparrow - N\downarrow}{N\uparrow + N\downarrow}$ spin polarization is high, it is possible to get a lower value of P_t due to significant difference in the Fermi velocities of spin and spin down bands,$v_F\uparrow$ and $v_F\downarrow$.

Chapter 3

Possibility of Spin triplet pairing in mesoscopic Pb-point contacts

3.1 Enhanced Superconductivity in Lead Point Contacts

The point contacts were made using a polycrystalline lead pellet and Silver tip(diameter 250 μm). The movement of the tip to fabricate the point contacts was controlled using a 100 threads per inch differential screw. The tip was pressed onto the sample to break through the oxidized layers.

It is know that Bulk lead is a conventional Superconductor with critical Magnetic field of about 800 Gauss [13]. However in our Point Contact experiments it was seen that the superconductivity in several point contacts survived upto high critical fields of 3 Tesla.

We have plotted differential resistance $\frac{dV}{dI}$ versus V_{DC}(potential difference across the junction) to analyse Andreev reflection spectra.

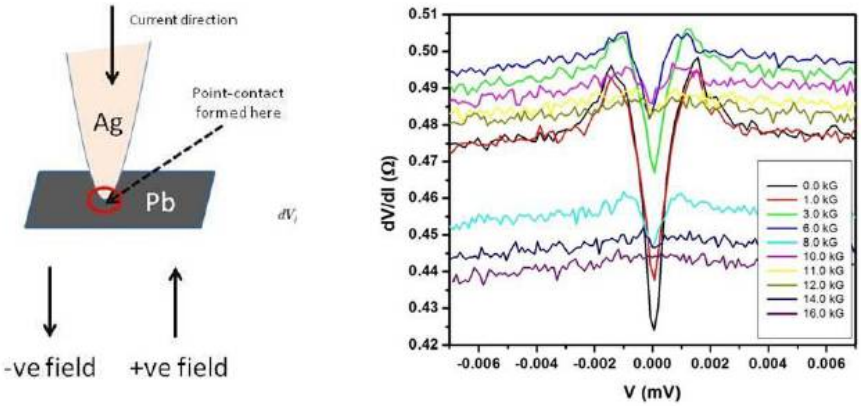

Figure 3.1: Pb-Ag point contact: (a)Experimental setup, (b)Thermal limit data of magnetic field dependence of $\frac{dV}{dI} spectra$

We can see in figure 3.1 the superconductivity survives upto 1.6 Tesla.This behaviour is similar to the enhanced critical magnetic field observed in lead nano-particles [33]. In our experiment, the point contacts could be compared to nano-domains trapped under the point contact. We estimated the constriction diameter using Wexler's formula for resistance of point contacts in the intermediate regime. All point contacts diameters varied between few nanometers.

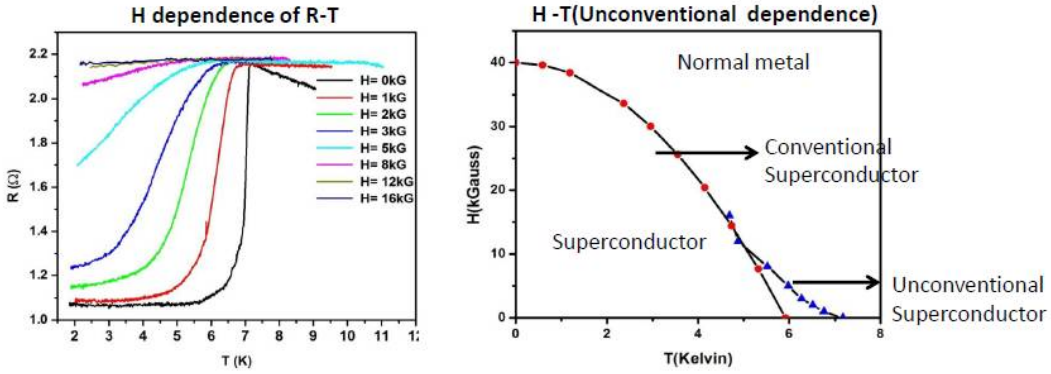

Figure 3.2: (a)Magnetoresistance of the point contact in firgure 3.1, (b)H-T diagram of the same point contact-Blue dots(Pb-Ag data), clearly show unconventional pairing, Red dots show a empirically expected H-T phase diagram of a conventional superconductor

Along with the Magnetic field dependence of differential conductance spectra, we also did the magnetoresistance(two probe resistivity measurement) of the same point contact (Figure 3.2). It can be seen from Figure 3.2 that critical temperature of the point contact reduces with increasing magnetic field. On plotting the $H - T$ graph, we observed that the H-T phase diagram has a significant deviation from that expected in a conventional superconductor. A possible reason for the unconventional $H - T$ dependence could be, since inversion symmetry breaks at the surface, it possible for the system to exist in mixed triplet state $s + ip$ [20], [7].

3.2 Asymmetry in Differential resistance

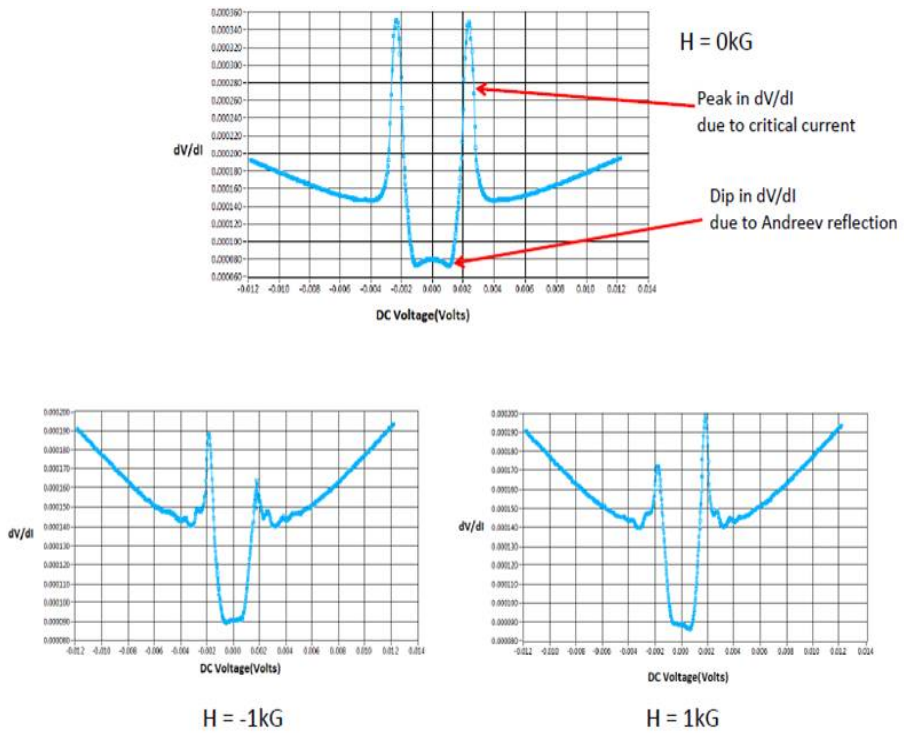

Figure 3.3: Pb-Ag point contact: In presence of magnetic field-Asymmtery(critical current peaks and Andreev features) in differential resistance with respect to the direction of potential bias across the junction

As shown in figure, 3.3 we observed that in presence of magnetic field, in differential resistance spectra, the height of critical current peaks and Andreev features is current direction dependent. There is a clear asymmetry in the resistance with respect to the positive and negative bias.

3.2.1 Behaviour in magnetic field

Experiments were also done on Lead with Cobalt tip. Similar results were observed in Pb-Co point contacts. As shown in figure 3.4, the asymmetry was clearly observed in both Pb-Ag (Figure 3.4(a)) point contacts and Pb-Co (Figure 3.4(b)) point contacts [4]. In addition to this, the direction of asymmetry laterally reversed on inverting the direction of magnetic field.

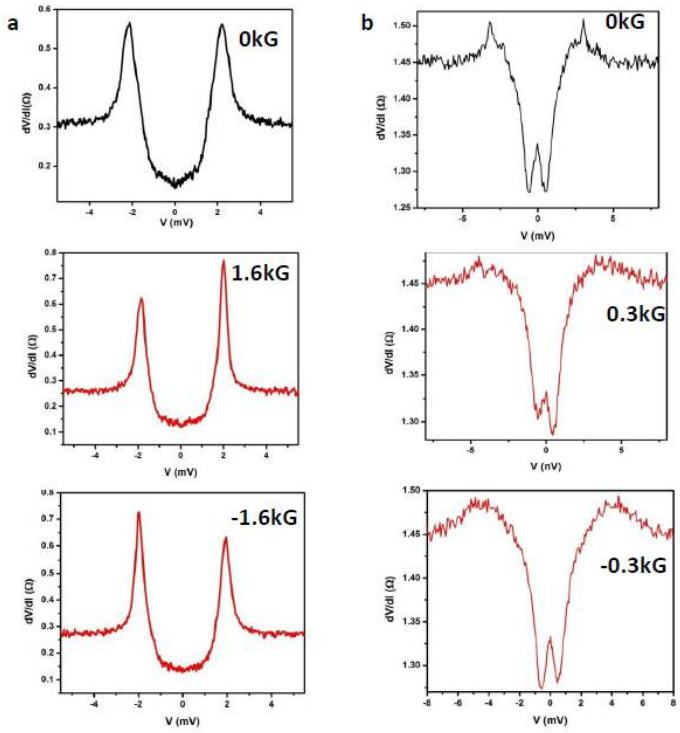

Figure 3.4: (a)Thermal limit Pb-Ag point contact showing asymmetry in presence of magnetic field, laterally reverses on inverting the direction of magnetic field, (b)Nearly ballistic limit Pb-Co point contact showing asymmetry in Andreev feature in presence of magnetic field

Since Lead is a heavy metal, it has high spin orbit coupling [3]. As time reversal symmetry breaks on applying magnetic field, it possible for such a state(s+ip) to couple with magnetic field, which we see in the spectra.

3.2.2 Oscillation in magnetic field

Another interesting feature was observed in the differential resistance spectra (Figure 3.5). As the magnetic field was increased, it was seen that the height of the critical current peaks oscillated, until they completely vanished with approaching critical magnetic field.

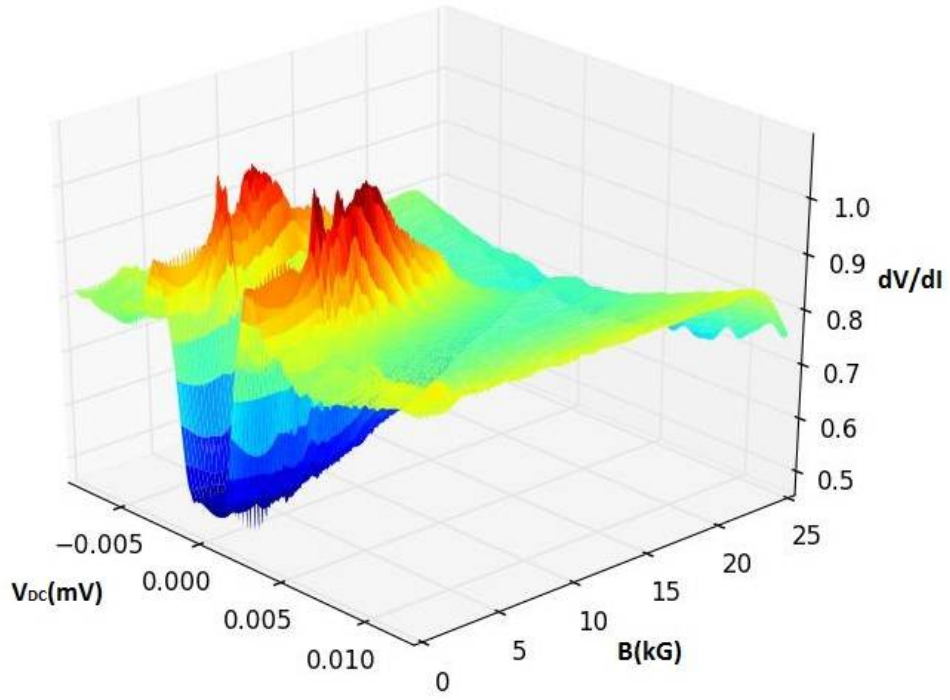

Figure 3.5: 3D diagram of diffusive limit Pb-Ag point contact showing oscillation in the critical current peaks with increasing magnetic field

Analysis

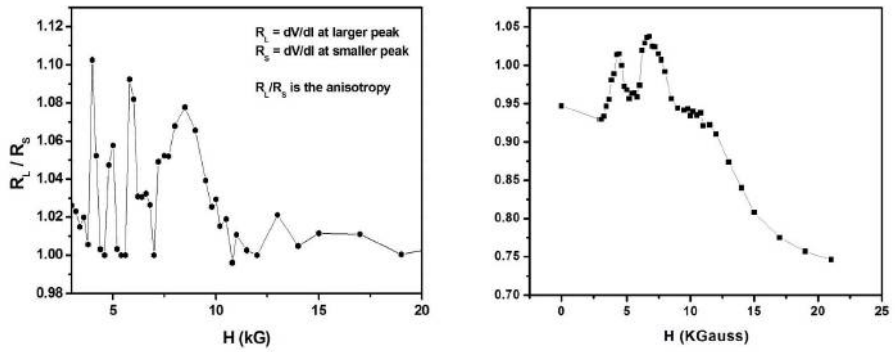

Figure 3.6: (a)ratio of R_L with R_S, (b)Differential resistance of Critical current of the positive bias with magnetic field

We have analysed the amount of asymmetry, by plotting in figure 3.6 (a) the ratio of the differential resistance of critical current peaks R_L and R_S with magnetic field, where R_L is the longer of the critical current peaks in a spectra and R_S the shorter one and in figure 3.6 (b)the differential resistance of the critical current peaks of the positive bias with magnetic field. Both the plots show clear oscillation.

We have not conclusively determined the reason for the asymmetry. Future work on this includes, solving the Hamiltonian of the system and checking if the state(s+ip) couples with magnetic field and indeed produces an asymmetry.

Bibliography

[1] A. A. Abrikosov. Nobel lecture: Type-ii superconductors and the vortex lattice*. *Rev. Mod. Phys.*, 76:975–979, Dec 2004.

[2] K. Ahilan, F. L. Ning, T. Imai, A. S. Sefat, R. Jin, M. A. McGuire, B. C. Sales, and D. Mandrus. Nmr investigation of the iron pnictide superconductor lafeaso 0.89. *Phys. Rev. B*, 78:100501, Sep 2008.

[3] J. R. Anderson and A. V. Gold. Fermi surface, pseudopotential coefficients, and spin-orbit coupling in lead. *Phys. Rev.*, 139:A1459–A1481, Aug 1965.

[4] T. Ando. Quantum point contacts in magnetic fields. *Phys. Rev. B*, 44:8017–8027, Oct 1991.

[5] J. Bardeen. Critical fields and currents in superconductors. *Rev. Mod. Phys.*, 34:667–681, Oct 1962.

[6] G. E. Blonder, M. Tinkham, and T. M. Klapwijk. Transition from metallic to tunneling regimes in superconducting microconstrictions: Excess current, charge imbalance, and supercurrent conversion. *Phys. Rev. B*, 25:4515–4532, Apr 1982.

[7] C. J. Bolech and T. Giamarchi. Point-contact tunneling involving low-dimensional spin-triplet superconductors. *Phys. Rev. Lett.*, 92:127001, Mar 2004.

[8] A. M. Duif, A. G. M. Jansen, and P. Wyder. Point-contact spectroscopy. *Journal of Physics: Condensed Matter*, 1(20):3157, 1989.

[9] A. G. M. Jansen, A. P. van Gelder, and P. Wyder. Point-contact spectroscopy in metals. *Journal of Physics C: Solid State Physics*, 13(33):6073, 1980.

[10] L. Janson, M. Klein, H. Lewis, A. Lucas, A. Marantan, and K. Luna. Undergraduate experiment in superconductor point-contact spectroscopy with a Nb/Au junction. *American Journal of Physics*, 80:133–140, Feb. 2012.

[11] C. Kallin and A. J. Berlinsky. Is sr 2 ruo 4 a chiral p-wave superconductor? *Journal of Physics: Condensed Matter*, 21(16):164210, 2009.

[12] J. R. Kirtley. Probing the order parameter symmetry in the cuprate high temperature superconductors by {SQUID} microscopy. *Comptes Rendus Physique*, 12(56):436 – 445, 2011. Superconductivity of strongly correlated systems Supraconductivit des systmes fortement corrls.

[13] R. Koepke and G. Bergmann. The upper critical magnetic field of lead as a function of the mean free path of the electrons. *Zeitschrift fr Physik*, 242(1):31–44, 1971.

[14] I. I. Mazin. How to define and calculate the degree of spin polarization in ferromagnets. *Phys. Rev. Lett.*, 83:1427–1430, Aug 1999.

[15] C.-Y. Moon and H. J. Choi. Chalcogen-height dependent magnetic interactions and magnetic order switching in $\mathrm{fese}_x\mathrm{te}_{1-x}$. *Phys. Rev. Lett.*, 104:057003, Feb 2010.

[16] S. Mukhopadhyay, P. Raychaudhuri, D. A. Joshi, and C. V. Tomy. Temperature dependence of transport spin polarization in Ndni_5 from point-contact andreev reflection. *Phys. Rev. B*, 75:014504, Jan 2007.

[17] Y. G. Naidyuk and I. K. Yanson. Point-Contact Spectroscopy. *ArXiv Physics e-prints*, Dec. 2003.

[18] B. Nikolić and P. B. Allen. Electron transport through a circular constriction. *Phys. Rev. B*, 60:3963–3969, Aug 1999.

[19] B. K. Nikolić and P. B. Allen. Resistivity of a metal between the boltzmann transport regime and the anderson transition. *Phys. Rev. B*, 63:020201, Dec 2000.

[20] M. Nishiyama, Y. Inada, and G.-q. Zheng. Spin triplet superconducting state due to broken inversion symmetry in li_2pt_3B. *Phys. Rev. Lett.*, 98:047002, Jan 2007.

[21] A. Plecenik, M. Grajcar, i. c. v. Beňačka, P. Seidel, and A. Pfuch. Finite-quasiparticle-lifetime effects in the differential conductance of $bi_2sr_2cacu_2o_y$/au junctions. *Phys. Rev. B*, 49:10016–10019, Apr 1994.

[22] B. Qian, J. Lee, J. Hu, G. C. Wang, P. Kumar, M. H. Fang, T. J. Liu, D. Fobes, H. Pham, L. Spinu, X. S. Wu, M. Green, S. H. Lee, and Z. Q. Mao. Ferromagnetism in cufesb: Evidence of competing magnetic interactions in iron-based superconductors. *Phys. Rev. B*, 85:144427, Apr 2012.

[23] B. Qian, J. Lee, J. Hu, G. C. Wang, P. Kumar, M. H. Fang, T. J. Liu, D. Fobes, H. Pham, L. Spinu, X. S. Wu, M. Green, S. H. Lee, and Z. Q. Mao. Ferromagnetism in cufesb: Evidence of competing magnetic interactions in iron-based superconductors. *Phys. Rev. B*, 85:144427, Apr 2012.

[24] M. Sargolzaei. First principles study on spin and orbital magnetism in cufesb and cucosb alloys with {C1b} structure. *Solid State Communications*, 150(3940):1861 – 1864, 2010.

[25] G. Sheet, S. Mukhopadhyay, and P. Raychaudhuri. Role of critical current on the point-contact andreev reflection spectra between a normal metal and a superconductor. *Phys. Rev. B*, 69:134507, Apr 2004.

[26] G. Sheet, H. Rosner, S. Wirth, A. Leithe-Jasper, W. Schnelle, U. Burkhardt, J. A. Mydosh, P. Raychaudhuri, and Y. Grin. High spin polarization in the ferromagnetic filled skutterudites Kfe_4sb_{12} and $Nafe_4sb_{12}$. *Phys. Rev. B*, 72:180407, Nov 2005.

[27] S. Singh, G. Sheet, P. Raychaudhuri, and S. K. Dhar. $CeMnNi_4$: A soft ferromagnet with a high degree of transport spin polarization. *Applied Physics Letters*, 88(2):022506, Jan. 2006.

[28] R. J. Soulen, J. M. Byers, M. S. Osofsky, B. Nadgorny, T. Ambrose, S. F. Cheng, P. R. Broussard, C. T. Tanaka, J. Nowak, J. S. Moodera, A. Barry, and J. M. D.

Coey. Measuring the spin polarization of a metal with a superconducting point contact. *Science*, 282(5386):85–88, 1998.

[29] R. J. Soulen, M. S. Osofsky, B. Nadgorny, T. Ambrose, P. Broussard, S. F. Cheng, J. Byers, C. T. Tanaka, J. Nowack, J. S. Moodera, G. Laprade, A. Barry, and M. D. Coey. Andreev reflection: A new means to determine the spin polarization of ferromagnetic materials. *Journal of Applied Physics*, 85(8), 1999.

[30] G. S. Thakur, Z. Haque, L. Gupta, and A. Ganguli. CuFeAs: A New Member in the 111-Family of Iron-Pnictides. *Journal of the Physical Society of Japan*, 83(5):054706, May 2014.

[31] M. A. Topinka, B. J. LeRoy, S. E. J. Shaw, E. J. Heller, R. M. Westervelt, K. D. Maranowski, and A. C. Gossard. Imaging coherent electron flow from a quantum point contact. *Science*, 289(5488):2323–2326, 2000.

[32] G. Wexler. The size effect and the non-local boltzmann transport equation in orifice and disk geometry. *Proceedings of the Physical Society*, 89(4):927, 1966.

[33] C. Yang, F. Tsao, S. Wu, W.-H. Li, and K. Lee. Enhanced critical magnetic field in superconducting pb nanoparticles. *Journal of Low Temperature Physics*, 131(3-4):349–352, 2003.